BIOMECHANICS AND BIOTRIBOLOGY OF ORTHOPAEDIC KNEE PROSTHESES

Lucian CĂPITANU, Luige VLĂDĂREANU, Justin ONIŞORU, Aron IAROVICI

This paper is a thorough analysis on the wear phenomenon of the total knee prosthesis, especially of the tibial tray insert of ultra-high molecular weight polyethylene (UHMWPE), due to cyclic biomechanical loading. The focus is on the evolution of the phenomenon, from adhesive wear pitting followed by delaminating and even breaking the insert. There are presented theoretical considerations regarding the non–conform contact between the femoral condyle and the tibial tray, experimental results, as well as the possibility to predict the fatigue wear of the UHMWPE tibial tray insert.

1. INTRODUCTION

Recent clinical studies (Blum et al. [1], Wasielievski et al. [2]) on massive wear of the tibial polyethylene insert caused by improper contact gear for the artificial knee joint, have shown that this is the main cause for the correction of the knee prosthesis. In paper [3], Knight et al. reports that in all of the 18-th worn prosthesis (out of 209 cases of primary arthroplasty for knee joint) we can observe wear pits on the surface of the tibial tray (specific to the adhesive wear) as well as delaminating. Prosthesis life was about 80 months, close to the time reported in [4], that is 72 months. There were also studies on the massive delaminating of the polyethylene occurred earlier (Engh et al. [5], Jones et al. [6], Kilgus et al. [7], Mintz et al. [8]). One case study (published by Ries et al. [9]), shows that is a correlation between polyethylene's massive wear and its delamination and the progress of crystallization in a plan concurrent with the failure plan, noticing at the same time an oxidation peak below the contact area of the UHMWPE inserts, air gamma-irradiation and aging.

The disputed idea that the wear of the polyethylene insert can be reduced by increasing of its thickness is rather false. In reality the main cause of the joint wear phenomenon is represented by the high level of the superficial pressure caused by incongruent contact areas ([3, 4]) and the present study is based on this idea.

One starts with a close analysis of the different types of tibio-femoral prosthetic joints: fixed bearing condylar prosthesis with a partial conformity between the tibial and femoral surfaces (over or exterior to the crossed posterior

Institute of Solid Mechanics – Romanian Academy, Const. Mille, 15, RO-70701

Rev. Roum. Sci. Techn. – Méc Appl., Tome 53, No. 3, P. 289–307, Bucarest, 2008

ligament) and mobile prosthesis with tibial component consisting in a fixed metallic tray with one/two plastic component/components defining the movement surface of the bearing. These components can have translational and rotational movements. There were also studies on prosthesis with a rotating tray, similar to those mentioned above, but where the plastic component of the bearing fulfil only one free rotation around the longitudinal axis, generally located in the centre.

Fig. 1 – Images of the total knee prosthesis components with fatigue wear.

Following the protocol signed with "Foişor" Orthopaedic Clinical Hospital from Bucharest, it was possible to analyze 20 total knee prosthesis (generally mobile bearing knee prosthesis) surgically removed. Macro and microscopic photo investigations on prosthesis (Fig. 1), showed that the most common wear is fatigue wear.

Insert on Fig. 2 comes from a prosthesis replaced far earlier than expected (after 67 months from the implant) because of tibial component migration.

In this case, fatigue wear had serious damage effects consisting in massive medial polyethylene loss and severe lateral delaminating. The qualitative analysis of the implants surgically removed reveals that tibial components presents at first adhesive pits on the contact area of the polyethylene insert and then delaminating (especially on the medial surface), in time resulting in massive damages on the polyethylene layer.

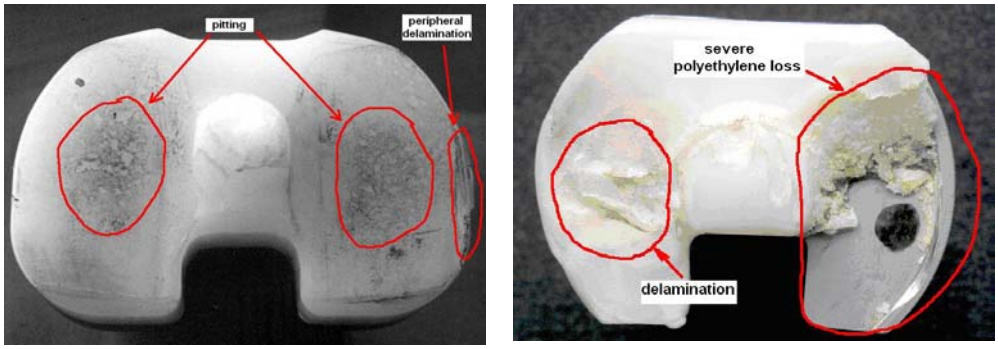

a b

Fig. 2 – Two replaced prosthetic components:
a) specific pits of adhesive wear; b) severe polyethylene insert delamination.

2. THEORETICAL AND EXPERIMENTAL STUDY OF ARTIFICIAL JOINT WEAR

The prosthetic knee joint must do flexion-extension movement (FE), antero-posterior translation (ATP) and internal-external rotation (IOR) during a cyclic loading. The first step for studying the total knee prosthesis wear was to analyze, from a theoretical and lab point of view, the experimental ball/plan couple during abovementioned movements. Regarding technical constraints, the loading value during the experimentation was considered stable.

Two bodies with a point contact area are deformed, when pressed one against the other, creating small areas of contact. Hertz calculated the strains and stresses produced inside the homogeneous and isotropic bodies. The established formula shows that on contact area is acting only normal stress.

For two bodies with elasticity modules E_1, E_2 and Poisson's coefficients ν_1, ν_2, one defines the equivalent elasticity module E, according to the following formula:

$$E = \frac{2E_1E_2}{\left(1-\nu_1^2\right)E_2 + \left(1-\nu_2^2\right)E_1}. \tag{1}$$

When taking into account the ball/plane couple, the ball being made of CoCr alloy with $E_1 = 1.9 \cdot 10^4$ daN/mm^2 and $\nu_1 = 0.3$ and the plane specimen made of UHMWPE with $\nu_2 = 0.36$ and $E_2 = 106$ daN/mm^2, it results an equivalent modulus $E = 242$ daN/mm^2.

A mutual compressive force F should create a contact spot by elastic deformation of the surfaces. For the Co-CR/UHMWPE couple, the plane surface is the most deformable creating an incongruous contact surface. Radius of the ball r_1 is different than radius r_2 of the deformed surface, so the equivalent radius of contact surface is:

$$r = \frac{r_1 r_2}{r_2 - r_1}. \tag{2}$$

The displacement h of the centre of the sphere, caused by its penetration into the plane specimen, is:

$$h = \left(\frac{9F^2}{4rE^2} \right)^{1/3}. \tag{3}$$

The diameter l of the deformed spherical calotte (Fig. 3) is expressed by the formula:

$$l = 2\left(\frac{3Fr}{2E} \right)^{1/3}. \tag{4}$$

The drawn hemisphere above the contact circle represents the compression stress distribution on the contact surface and the maximum stress value σ_{ma} is:

$$\sigma_{\max} = \frac{6F}{\pi l^2}. \tag{5}$$

The maximum shear stress occurs at the edge of the contact area and has the following value:

$$\tau_{\max} = \frac{1 - \nu_2}{3} \sigma_{\max}. \tag{6}$$

For ductile materials, the maximum shear stress is very important and it occurs in both contact bodies at a depth of ¼ below the centre of the contact circle. At a value of $\nu_3 = 0.3$ one has $\tau_{\max} = 0.3\ \sigma_{\max}$.

Fig. 3 – Hertzian contact of the coupling ball/plane.

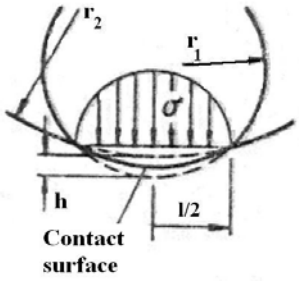

The experimental device, for studying the wear process on the components of total knee prosthesis, uses a ball/plane couple. This is composed of a ball made of a Co-Cr alloy, imitating a condyle of the femoral component and a polyethylene plane disk of UHMWPE (having a thickness of 5 or 10 mm), placed right under it.

The tri-axial movements consisted of flexion-extension movements (FE), antero-posterior translation (ATP) and internal-external rotation (IOR). The FE movement has been induced to the ball and the APT and IOR movements have been induced to the disk (Fig. 4). These movements were made by a crank gear mechanism.

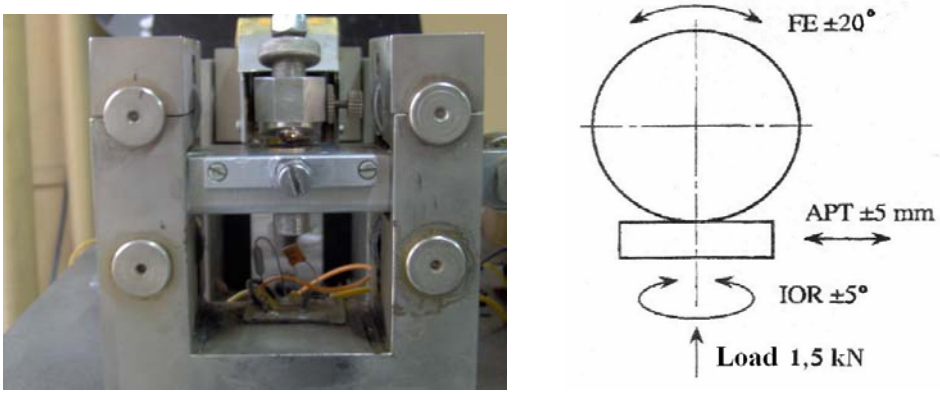

Fig. 4 – Image of the experimental apparatus and friction coupling kinematics.

The testing device is similar to that used at Helsinki University Technology by V. Saikko, T. Ahlroos and O. Calonius [10]. The variation of the movements in time was almost sinusoidal, the duration of the cycle of movements is of 1 *s* and the amplitude of the FE movement was of 40^0. If the FE movement would have been the only movement occurred during the process, the sliding distance between the extremities would have been of about 20 mm, for a ball 54 mm diameter. Still, the APT movement of 10 mm amplitude was synchronized with the FE movement, so that the maximum flexion would coincide with the maximum anterior translation of the disk, while the maximum extension would coincide with the maximum posterior translation. As a result, the sliding distance between the

extremities, was reduced. Due to the APT movement the contact spot has a cyclic movement on the disk.

The crank gear mechanism has been made in such a way that the difference in phase of the IOR and APT sinusoidal waves should reach the value $\pi/2$. Consequently the point of application of the force on the disk (referring to the course of a theoretical contact point) represents a symmetrical narrow figure, eight-form, at a 9.42 mm length and 0.22 mm width. The length of this curve of the was about 18.84 mm and this value served in the calculation of the wear factor for one cycle sliding distance.

The APT movement was realised in order to permit the lever fixed on the FE shaft to produce the displacement of a linear horizontal guide at a inferior friction force. It is connected at a force transducer and the signal was proportional to the friction force between the ball and the disk. In this way one can calculate the friction coefficient μ. Due to a substantial indent of the ball into the disk, considering the viscoelastic properties of the polyethylene, a more adequate term to use is the coefficient of the total kinetic resistance [11].

The first measurements made, using FE and APT biaxial movements, lead to inferior wear rate. Adding IOR movements the wear rate increased. For 10^0 IOR amplitude, the IOR axis is the vertical symmetry axis of the disk. The results refer to the output of the application of IOR and APT movements only, when the wear indentation is linear. The FE movements adding give a more complex wear phenomenon.

Many studies demonstrate that the load on bearing it needn't necessarily be dynamic, so that we considered a vertical and static force of 1.5 kN and we supposed this piece of information available also for the knee. Due to APT the stresses inside in the disk presents a cyclic variation.

In fact, the ball made from Co-Cr alloy with a 54 mm diameter, consisted of a modular femoral head taken from a partial hip prostheses. The axis of the ball holder (similar to the stem prosthesis) has been placed at a 45° from the main axis of the tiller plate. Thus it was possible to use the same ball at more than one test by fixing it each time in a different position. The ball was properly centred so that it fall right on the FE axis. The underside of the disk was fixed on a plane head made of Co-Cr alloy.

Disk tests were made of high density polyethylene type GUR 1050. There were made five experiments on disk tests, having 40 mm diameter. The aging behaviour of polyethylene disks has been made by gamma irradiation in air.

As lubricant it has been used normal saline sterilized solution, in three parts filtered 0,1 μm, with a low level of proteins and endotoxines, diluted 1:1 and free from additives. The quantity of lubricant in the acrylic testing pot was of 200 ml. The pot was deliberately big and open, in order to prevent overheating that might affect the wear simulation. Tests were undertaken at the room temperature and the temperatures near the pot, as well as the lubricant's temperature, were checked daily. During the experiments the value of the friction force was also registered.

Each test took eight weeks and about $5 \cdot 10^6$ cycles and occurred at a 1 Hz frequency. Tests had been stopped at 500,000 cycle's intervals in order to change the lubricant. Meanwhile the tests were interrupted, the specimens and the plates were water-flushed. At the end of the test, the disk was dehydrated in a vacuum for 30 minutes. The maximum contact pressure values were calculated assuming that the contact diameter was equal with the width of the worn area, while the distribution of the contact pressure was elliptical.

3. THEORETICAL WEAR MODELLING

The wear tests on the UHMWPE plane component, applying only IOR and APT movements, point out signs of wear, as it can be seen in Fig. 5. The external sizes of the impression (length = L and width = l) have been measured with an electronic microscope when each test was finalized. The depth of the impression had been calculated in this case by ink copy technique, because it can not be measured with a profilometer or by feeling, as a result of polyethylene reduced hardness. It consisted of pressing the polyethylene specimen against the ink copy paper creating the possibility to outline the contour of the wear.

Considering the rigidity of the ball one obtains a relative uniformity for the bottom of the impression, this could be considered as the sum of cylinder sectors of equally length p (Fig. 5).

In this case, the lateral surface of one cylinder sector is given by the following relation:

$$S_i = 0.5r^2(\pi\varphi_i/180 - \sin\varphi_i), \tag{7}$$

where: φ_i – angle at the centre, r – circular sector radius .

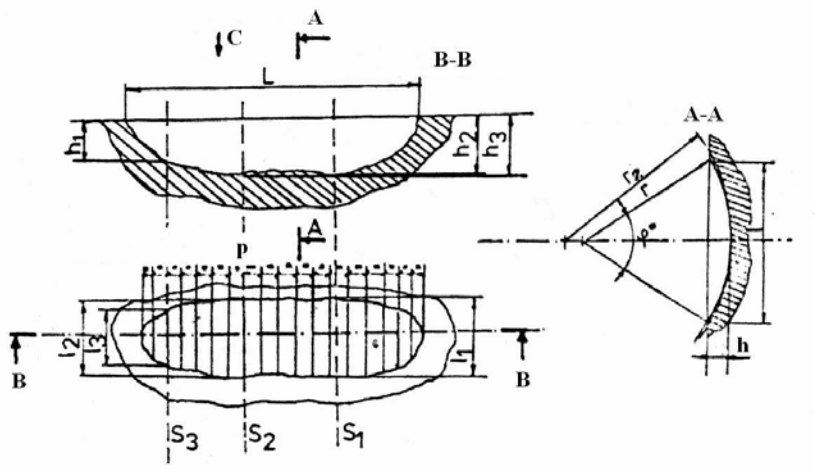

Fig. 5 – The form of the wear on the plane component.

The radius r can not be identified, inside the material of metal/plastic couple, with the circular radius. This is caused by the great elastic deformations of the polyethylene disk, leading to an extension of its radius in the contact area. This aspect is briefly presented and illustrated in Fig. 6.

At a r_1 – radius of unstrained contact area and r_2 – radius of strained contact area, we can observe, from Fig. 6b, that $r_2 > r_1$.

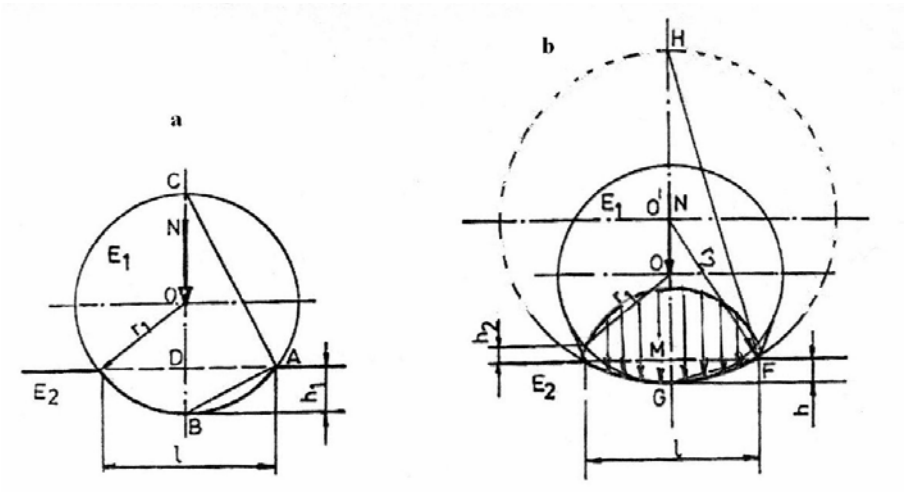

Fig. 6 – Elastic deformation under load of the plane component, in the contact area: a) theoretical case; b) practical case.

The increasing of the contact area radius implies the decreasing of depth imprint, from h_1 value (Fig. 6a) to h value (as in Fig. 6b), at a h_2 quantity:

$$h_2 = h_1 - h \,. \tag{8}$$

From ABC triangle, it results:

$$h_1(2r_1 - h_1) = l^2/4 \,.$$

The depth h_1 is very low so h_1^2 is a negligible value, comparing to the other measurement's quantities, and thus one obtains:

$$h_1 = l^2/8r_1 \,. \tag{9}$$

In the same way from FGH triangle it results:

$$h(2r_1 - h) = l^2/4 \,.$$

Operating in a similar way:

$$h = l^2 / 8r_2 \ . \tag{10}$$

On the basis of the abovementioned relations, it results:

$$h_2 = l^2 (r_2 - r_1) / 8r_1 r_2 = l^2 / 8r \ . \tag{11}$$

where r is the equivalent contact radius from (2).

Relation (11) becomes:

$$r = l^2 / 8h_2 \ . \tag{12}$$

Considering the friction couple loaded in elastic field and an elliptical stresses distribution, by calculating the wear impression width, we obtain the following Herzian relation:

$$l^2 = 32F \cdot r(1 - \nu^2) / (\pi E \cdot L) \ . \tag{13}$$

Considering the wear impression as being formed out of a sum of cylinder sectors, by a serial extension of the relation (7), omitting high powers, the reduction of the angle as well as replacing the centre angle by the ratio *l/r*, for lateral surfaces of one sector we have:

$$S_i = l_i^3 / 12r_i \,, \tag{14}$$

where r_i represents the equivalent contact radius in the point of width l_i. Neglecting the non-uniformity of the impression, (14) becomes:

$$S_i = l_i^3 / 12r \ . \tag{15}$$

Taking into account relation (2) and (12), it results that:

$$S_i = 2l_i \cdot h / 3 \ . \tag{16}$$

The volume of the material, replaced because of extended wear, will become:

$$V_u = \sum_{i=1}^{n} (S_{i \cdot} p_i) = 2l_m \cdot h_m \cdot L / 3 \,, \tag{17}$$

where (l_m) is the medium width of the wear impression, h_m is the medium depth and L its length.

On the basis of relation (3) it results that:

$$h^3 = \left(r_2 - r_1\right)^3 = \frac{9F^2 \left(r_2 - r_1\right)}{4E^2 r_1 r_2} \ , \tag{18}$$

whence:

$$4E^2 r_1 r_2 \left(r_2 - r_1\right)^2 = 9F^2 . \tag{19}$$

The numerical work out will give the solution:

$$r_2 = 27.3212\,\text{mm} \cong 1.012 r_1 .$$

From a practical point of view, it is necessary to measure at the microscope the impression width in five pre-established points, calculating then the medium width of the wear impression. The resulting value will help when calculating the worn material volume from the plane component from V_u and the average depth of the wear out layer h_{mu}.

The results of the experiments, at a constant force of 1.5 kN , $\pm 5^0$ IOR movement and ± 5 mm APT, are presented in Table 1. Results of the test 1 and 2 were obtained on the polyethylene disks with 5 mm thickness, while those from test 3, 4, 5 were obtained on 10 mm thickness of the disks. For every movement cycle, the route length of the contact spot was 10 mm. The microscopic measurements showed an obvious increase of these values probably due to the shear stresses in the lateral contact area.

Table 1

Wear of polyethylene disks and average of friction coefficient

No	Wear [10^{-3} mm^3]	Wear factor [10^{-11}mm^3/Nm]	Wear pit dimensions			μ
			Length [mm]	Width [mm]	Depth [10^{-3} mm]	
1	72.258	0.935	10.3	1.32	0.6	0.036
2	128.559	1.697	10.1	1.61	1.3	0.053
3	71.311	0.914	10.4	1.31	0.5	0.035
4	120.399	1.514	10.6	1.55	0.9	0.034
5	112.475	1.428	10.5	1.52	1.0	0.047

During test 2 and 3, the UHMWPE specimens were sterilized by irradiation γ and aged by aerial convection. During test 1 and 4 were used non-irradiated specimens and test 5 occurred on irradiated and non-aged specimens.

The wear factor was set according with Archard relation [11]:

$$V_u = k \cdot F \cdot v \cdot t , \tag{20}$$

where: V_u – wear material volume; F – working load; v – relative sliding velocity; t – operating time; k – wear factor.

Dividing both terms in the relation (20) with nominal contact area A, we obtain:

$$h_u = k \cdot p \cdot v \cdot t , \tag{21}$$

whence: h_u – depth of the wear imprint [cm]; p – nominal contact surface pressure [daN/ cm^2].

Because the distance covered during a friction cycle is $L_f = v \cdot t$ one obtains :

$$k = h_u /(p \cdot L_f) \ , \tag{22}$$

respectively:

$$k = V_u /(F \cdot L_f) . \tag{23}$$

The tests made for different number of cycles demonstrated that wear velocity of disks, γ irradiated and aged by aerial convection, had at the beginning a higher value, then dropped and finally stabilized around the values of the non-irradiated wear velocity. Wear velocity of disks, γ irradiated and aged of 10 mm thickness, is roughly twice higher than that of non-irradiated disks at the same thickness value.

The wear speed of the 5 mm disks that were also aged is about 52 times higher than that of similar disks with a 10 mm thickness.

It's very difficult to evaluate the clinical wear of the tibial tray at the total knee prosthesis, due to considerable polyethylene creep. At the same time, it is difficult to establish the value of the wear factor because of the impediments faced when measuring the removed material volume.

4. FATIGUE WEAR PREDICTION OF THE KNEE PROSTHESIS COMPONENTS

The study of kinematics of the joint surfaces and the contact mechanism is very important for the diagnosis and the joint therapy, for a reasonable projection of the joint prosthesis as well as when studying the stability and the degeneration of the joint wear (artificial joint) or the degeneration of cartilage (natural joint). Furthermore, the relative analysis on the movement between the joint surfaces together with the kinematics of the body components, are decisive factors in the human body kinematics estimation.

Generally, any type of joint has six degrees of freedom (three translations along the axes of the attached Cartesian system and three rotations around the same axis) in a permittivity range of movements determined by the presence of intrinsic joint stabilizers – contact areas, or extrinsic – ligaments, synergic muscles, synovial membrane. That is why we can consider each of the human joints as a compromise between stability and movement, specially determined by the geometry of the joint surfaces.

When talking about knee joint, the width of the tibial tray is much bigger than that of the condyles (medial or lateral) but its length is much smaller, which leads us to conclusion that in case of large flexion there has to be antero-posterior movement. The medial area of the tibial tray is concave (with a radius of about 80 mm) and the lateral area is convex (radius of about 70 mm). The non-conformity of the joint

surfaces is decreased by the presence of the meniscus (gradually used when dealing with strong compressive forces).

Artificial joints are more simplistic, both areas of the tibial tray being concave and the default of the meniscus lead to the formation of new but limited contact area with high pressure contact areas in case of excessive compressive forces. In practice, the joint has 3 degrees of freedom – flexion/extension in the sagittal plane (the main rotation movement around the axes from Fig. 7), combined with a tibial antero-posterior translation movement and its internal/external rotation movement (around the frontal axis of the bone). The presence of the prosthesis implies the same active elements (muscular) and preservation of joint stabilizers, which lead us, if the natural character of the movement is maintained, to a certain form of the joint surfaces.

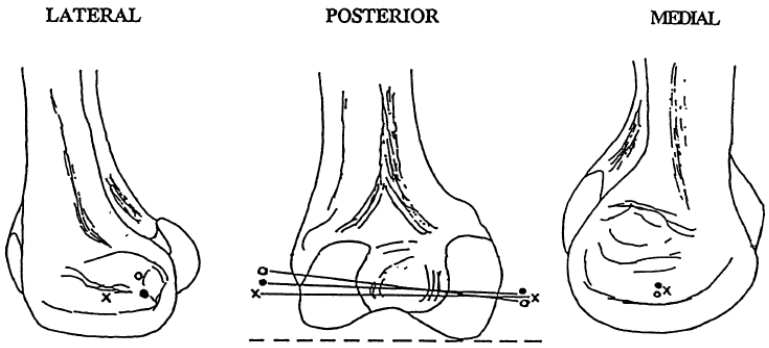

Fig. 7 – Rotation axes for flexion/extension movements.

In order to determine the kinematics of the artificial joint, under flexion/extension and antero-posterior translation, we performed a 2D study. Fig. 8a presents the different stages of the extended flexion movement. The curves from Figs. 8b-8d show the kinematics of the three marked points according to Fig. 7 – the three curvature points of the condylar surfaces.

The method, used for fatigue wear prediction of the tibial polyethylene insert in case of loading during the active cycles of movement, combines the results obtained by FEM, using a technique of summing up the effects of significant daily activities in order to calculate a cumulative wear assessment.

All the analyses used the FE model presented in Fig. 9, which includes a femoral condyle and a half (medial one) of the polyethylene insert and the metallic tibial tray. For the elastic components we have been used brick type elements with 8 nods and 3 degrees of freedom per nod (the three translations). The femoral condyle (which is considered to be rigid) has a toroidal form with a curvature radius of 22 mm in sagittal plane (the flexion plane) and a radius of 30 mm in frontal plane.

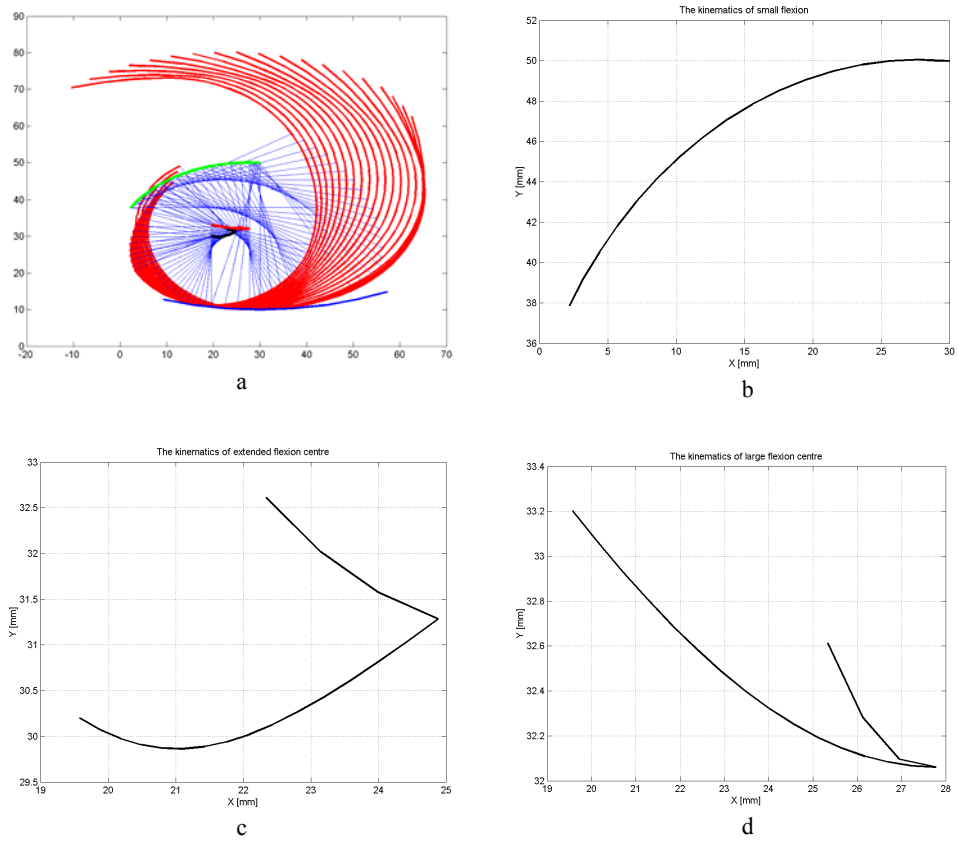

Fig. 8 – Kinematics of flexion/extension:
a) kinematics of the joint surfaces; b) the movement of the condylar surface centre for angles of small flexion; c) the movement of the condylar surface centre for large flexion angles; d) movement of the condylar surface centre for extended flexion

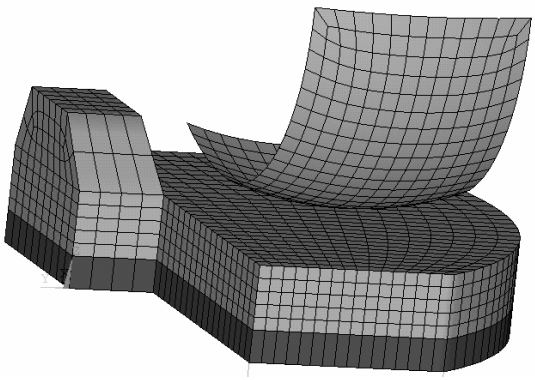

Fig. 9 – The model used for FE analysis.

The metallic and polyethylene components are supposed linear-elastic, having the mechanical characteristics values, mentioned in Table 2.

Table 2

Mechanical properties of the materials

Material	Longitudinal elasticity module [GPa]	Poisson Coefficient	Observations
Co-Cr alloy	200	0.3	from ISO 5832-4
UHMWPE	1.06	0.36	from Lewis [12]

Common daily activities which are considered relevant to the present study are normal walking and climbing or descending stairs.

The kinematics of the abovementioned movements can be seen in Fig. 10, which presents the segmental movement of the lower limb, as determined by Bergmann et al. [12] using a tandem movement system with one experimental telemetric prosthesis. Figure 10d presents the variations of the contact force for all major daily activities (Taylor and Walker, [13]). In Figs. 10e–f you could see the variation of the major movements ,flexion angle and intern-external rotation angle (Bergmann et al. [12]).

The compressive joint force is applied through the tibial tray (acting as a uniform distributed load at the bottom of it). The two rotation movements (flexion/extension and intern/external rotation) are applied as dynamic constraints of the femoral condyle movement. We considered that, for a maximum level of the flexion of about 70 degrees, antero-posterior translation is small (usually important in case of excessive ligament flexion as a result of a large flexion angles) and it can be neglected.

The contact mechanism between joint surfaces – the toroidal condylar surface and the plane surface of the tibial insert – is a combination between rolling and sliding.

It had been considered a friction law of Coulomb's type, with a constant friction coefficient $\mu = 0.12$ (Villa et al. [14]).

For every activity it was calculated the value of the wear factor, based on the variation of the maximum shear stress (see Sathasivam and Walker, [15]):

$$D_f^k = \sum_{i=1}^{n} \frac{1}{2} \left| \tau_{i+1} - \tau_i \right| \cdot \left(\left| \tau_{i+1} \right| + \left| \tau_i \right| \right), \tag{24}$$

where: D_f^k – wear factor for activity k; τ_i – maximum shear stress at time t_i.

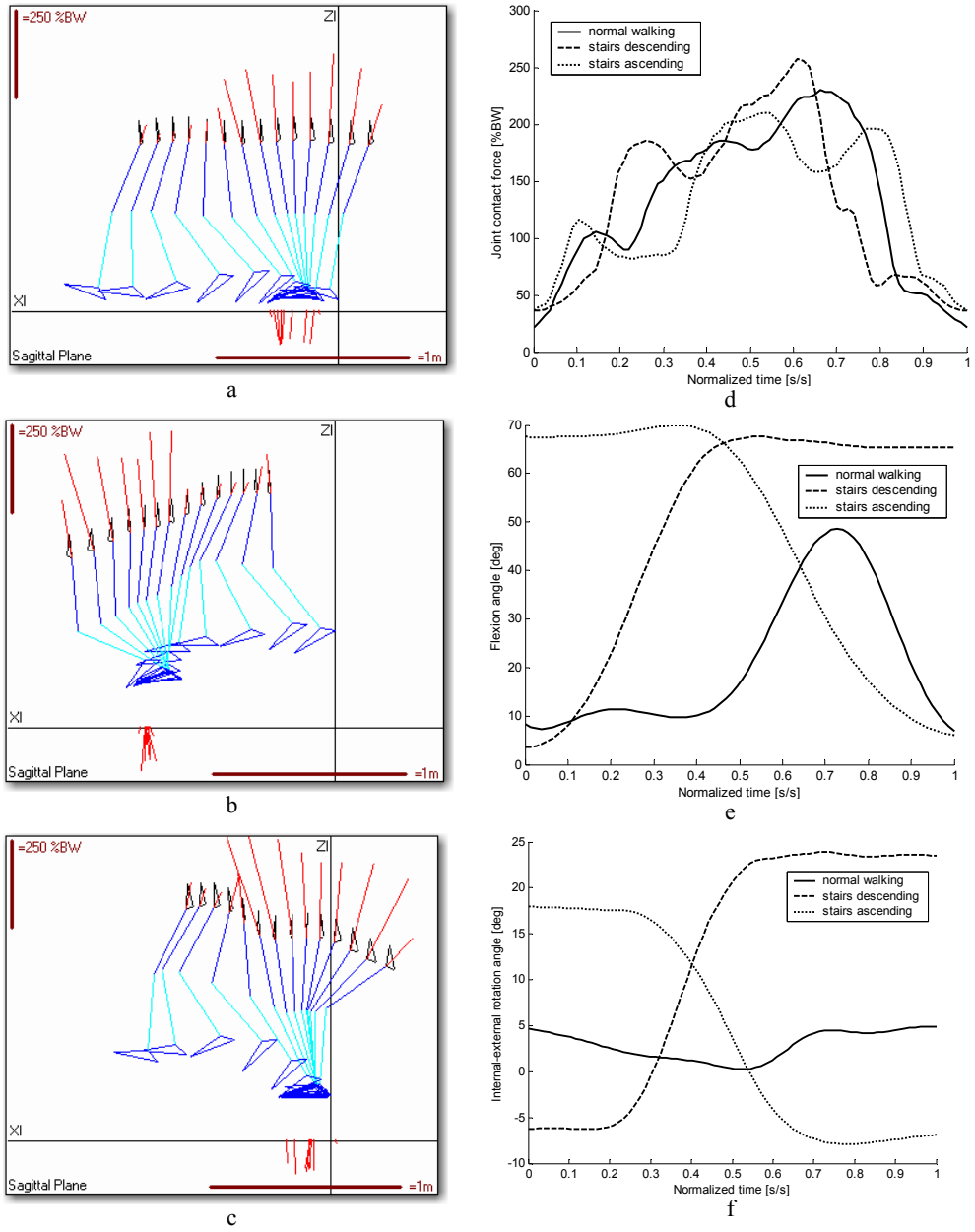

Fig. 10 – Dynamic conditions for analyzed daily activities.
Kinematics of the lower limb [12]:
a) normal walking, b) stairs descending, c) stairs climbing; Joint forces [13]: d) contact force;
Kinematics [12] of the joint surfaces:
e) flexion angle, f) internal-external rotation angle.

The effect of all the activities considered can be added up by using the weighted sum:

$$D_f^{tot} = \sum w_k D_f^k , \tag{25}$$

where the weight are functions that depends on the frequency of each activity apart.

5. RESULTS AND CONCLUSIONS

The dynamic analyses of the prosthetic joint contact (described in the previous section) permit to determine the characteristics of the load transfer mechanism inside the knee artificial joint. For example (Fig. 11) we can set the trajectory of the contact pole for the three mentioned activities.

The examination of these trajectories let us see that all deemed activities doesn't involve knee extension, which lead us to conclusion that only median and posterior areas of the insert will be stressed. For normal walking, the trajectory represents a closed curve, similar to the hysteretic curve. The other two activities have similar trajectories (but with different directions) with large intern/external rotation movements (when climbing the stairs at the beginning of the movement and for descending at the end of it). We can observe that while normal walking will constantly damage the median area of the polyethylene insert, climbing and descending the stairs will reach loading maximum values in the posterior area of tibial component.

Obviously, because of the joint surfaces geometry (condylar surface with toroidal shape and plane surface of the insert), the contact surface area will be an elliptical one with a major axis normal to the sagittal plane. The maximum contact pressure for each time interval could be a good estimator for the loading intensity inside the joint. Variation in time of the size will follow the have the same trajectory with that of the intensity variation (Fig 12).

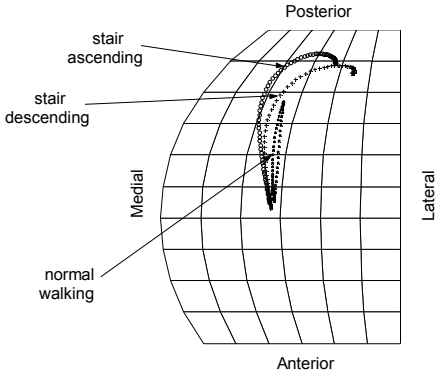

Fig. 11 – Trajectories of contact pole for deemed activities.

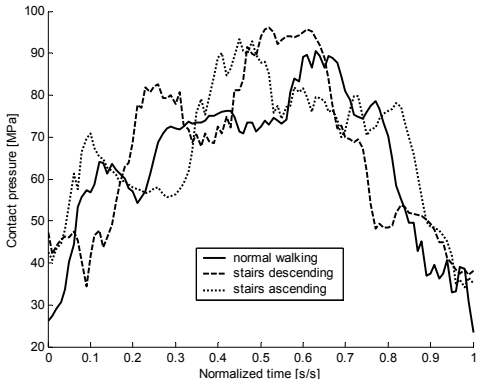

Fig. 12 – Variation of the contact pressure.

For all activities, it can be seen the existence of a rapid loading growing, up to a maximum value (corresponding to the initial contact between the leg and the ground) followed by a large period of time when the loading value remains almost unchanged (corresponding to body weight loading).

Even if the contact pressure is an important estimator for the loading level and for the resulting wear phenomenon, a better estimator for the fatigue wear will be the maximum shear stress (see relation (24)). From the contact mechanism (rolling and sliding combination) it results that maximum shear stress is located below the contact area at a depth depending upon the ratio between axes length of contact ellipse.

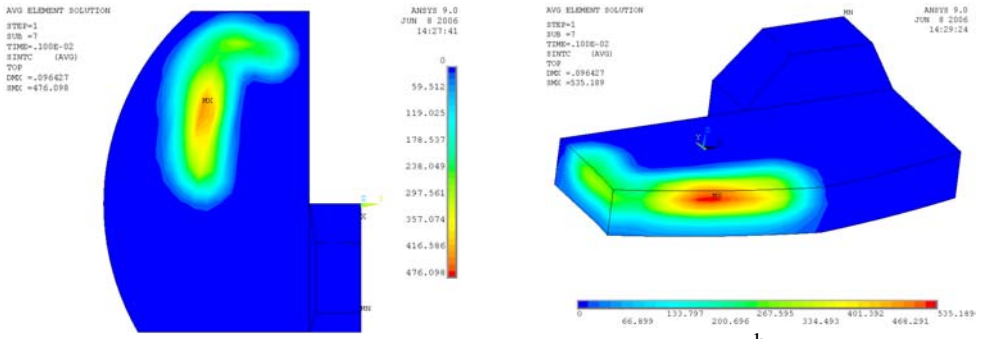

a b

Fig. 13 – Distribution of the wear factor: a) on the contact area, b) interior of the insert.

Using relation (25) one determines areas with a higher risk of initiation and increasing of wear, areas presented in Fig.13. The most affected areas of the polyethylene insert are the median and posterior ones. It also can be noticed that maximum wear probably starts inside the insert under the contact area which concurs with the clinical remarks regarding the beginning of severe delaminating.

Maximum values of the wear estimator (~477 MP^2 on the insert surface and ~535 MP^2 inside of it) are in conformity with the results reported by Sathasivam and Walker in [16] that reached prediction values of ~230 MP^2 for a constant loading of 1,000 N (approx. 120% BW).

In order to determine the occurrence of wear in high risk areas, the study presents a predictive method by combining the Finite Element Method evaluation of contact mechanism and transfer of load in articulation with a summation technique based on a damage estimator (damage score estimation).

Fatigue wear was identified as the main phenomenon responsible for massive wear of the polyethylene insert. Clinical studies shown that even for tibial components retrieved for different reasons (migration of the implant, creep etc.) there could be observed obvious signs of fatigue wear (cracks under the contact

area, pitting, delaminating, large polyethylene pieces detachments). The computed surface of cumulative maximum damage, that traverse the layers of the UHMWPE insert could be identified as the cracking surface in retrieved prostheses.

The cumulative nature of the fatigue wear phenomenon need a qualitative and quantitative evaluation of the transfer mechanism of loading through the joint and a summation technique for encountering the diversity of the human activities. The first action is to run a dynamic analysis on the models with finite elements. The second requirement involved three activities (normal walking, climbing and descending the stairs respectively). Thus, dynamic analyses were made on each activity, being possible to calculate the value of a wear factor (or damage score) and based on this were determined the high risk areas. These are located in an area were other studies (Ries et al. [9]) identifies an increase of the crystallisation percentage and the presence of subsurface oxidation peak, induced by gamma irradiation and ageing of the prosthesis. From the distribution of cumulative indicators (as in Fig. 6) we could notice that the wear areas are localised in the middle of the medial and posterior areas of the tibial insert. Ascending or descending stairs are considered activities that generate a large contact pressure but, due to its great frequency, normal walking is dominant.

This study could be extended in two directions: first one, by considering a larger field of activities and the influence of there frequency appearance on the loading (this situation was already obtained for hip joint prosthesis [12]); secondly, by improving the contact mechanism considering the viscoelastoplasticity of the polyethylene and by adopting some complex friction laws.

Received on March 24, 2008

REFERENCES

1. Blunn G.W., Joshi A.B., Minns R.J. et all, *Wear in retrieved condylar knee arthroplasties*, Journal of Arthroplasty, **12**, pp. 281-290, 1997.
2. Wasielewski, R.C., Galante, J.O., Leighty, R.M., Natarajan, R.N., Rosenberg, A.G., *Wear patterns on retrieved polyethylene tibial inserts and their relationship to technical considerations during total knee arthroplasty,*. Clinical Orthopaedic, **299**, pp. 31–43, 1994.
3. Knight, J.L., Gorai, P.A., Atwater, R.D., Grothaus, L., *Tibial Polyethylene Failure After Primary Porous-coated Anatomic Total Knee Arthroplasty*, Journal of Arthroplasty, **10**, pp. 748-757, 1995.
4. Heck, D.A., Clingman, J.K., Kettelkamp, D.G., *Gross polyethylene failure in total knee arthroplasty*, Orthopedics, **15**, pp. 23ff, 1992.
5. Engh, G.A., Dwyer, K.A., Hanes, C.K., *Polyethlyene wear of metal-backed tibial components in total and unicompartmental knee prostheses*, J Bone Joint Surg, **74B**, pp. 9-17, 1992.
6. Jones, S.M.G., Pinder, I.M., Moran, C.G., Malcolm, A.J., *Polyethylene wear in uncemented knee replacements*, J Bone Joint Surg, **74B**, pp. 18-22, 1992.
7. Kilgus, D.J., Moreland, J.R., Finerman, G.A., et al, *Catastrophic wear of tibial polyethylene inserts*, Clin Orthop, **273**, pp. 223-231, 1991.
8. Mintz, L., Tsao, A.K., McCrae, C.R., et al, *The arthroscopic evaluation and characteristics of severe polyethylene wear in total knee arthroplasty*, Clin Orthop, **273**, pp. 215-222, 1991.

9. Ries, M.D., Bellare, A., Livingston, B.J., Cohen, R.E., Spector, M., *Early Delaminating of a Hylamer-M Tibial Insert*, The Journal of Arthroplasty, **11**, pp. 974-976, 1996.
10. Saikko, V., Ahlroos, T., Calonious, O., *A three- axis Wear Simulator with ball-on-flat Contact,* Wear, **249**, pp. 310-315, 2001.
11. Archard J.F., *Contact and Rubbing of flat Surfaces*, J. Appl. Phys., **24**, pp.438-455, 1953.
12. Bergmann G., Deuretzbacher G., Heller M., Graichen F., Rohlmann A., Strauss J., Duda G.N., *Hip Contact Forces and Gait Patterns from Routine Activities,* Journal of Biomechanics, **34**, p. 859-871, 2001.
13. Taylor, S.J.G., Walker, P.S., *Forces and moments telemetered from two distal femoral replacements during various activities*, Journal of Biomechanics, **34**, pp. 839-848, 2001.
14. Villa T., Migliavacca F, Gastaldi D., Colombo M., Pietrabissa R, *Contact stresses and fatigue life in a knee prosthesis: comparison between in vitro measurements and computational simulation*, Journal of Biomechanics 37, pp. 45-53, 2004.
15. Sathasivam S., Walker P.S., *The conflicting requirements of laxity and conformity in total knee replacement*, Journal of Biomechanics, **32**, pp. 239-247, 1999.
16. Onisoru J., Capitanu L., Iarovici A., Popescu M., *A method for predicting the wear of the artificial joints*, Journal of Biomechanics, **39** (Suppl 1), S141, 2006.
17. Onisoru J., Capitanu L., Iarovici A., *Experimental wear prediction of a tibial tray of total knee Prostheses*, Polytechnic Institute Bulletin (Iaşi), Tome LII(LVI), Fasc. 6B, 2006.
18. Onisoru J., Capitanu L., Iarovici A., *Kinematics and contact in Total Knee Prostheses during routine activities*, Proceedings of SISOM, Bucharest, 2006.
19. Onisoru J., Capitanu L., Iarovici A., Popescu M., *Failure of a Tibial Insert of a Total Knee Prosthesis Due to Fatigue Wear*, Polytechnic Institute Bulletin (Iaşi), Tome LII(LVI), Fasc. 6A, 2006.
20. Popescu M., Capitanu L., *Proteze totale de şold. Inginerie şi ortopedie*, Edit.Bren,Bucureşti, 2006.